

OPEN ACCESS

EDITED BY

Alessandro Martorana,
University of Rome Tor Vergata, Italy

REVIEWED BY

Caterina Motta,
Santa Lucia Foundation (IRCCS), Italy
Francesco Di Lorenzo,
Santa Lucia Foundation (IRCCS), Italy

*CORRESPONDENCE

Mostafa Mehdipour Ghazi
✉ ghazi@di.ku.dk

RECEIVED 27 November 2023

ACCEPTED 12 February 2024

PUBLISHED 26 February 2024

CITATION

Mehdipour Ghazi M, Selnes P, Timón-Reina S,
Tecalão S, Ingala S, Bjørnerud A,
Kirsebom B-E, Fladby T and Nielsen M (2024)
Comparative analysis of multimodal
biomarkers for amyloid-beta positivity
detection in Alzheimer's disease cohorts.
Front. Aging Neurosci. 16:1345417.
doi: 10.3389/fnagi.2024.1345417

COPYRIGHT

© 2024 Mehdipour Ghazi, Selnes,
Timón-Reina, Tecalão, Ingala, Bjørnerud,
Kirsebom, Fladby and Nielsen. This is an
open-access article distributed under the
terms of the [Creative Commons Attribution
License \(CC BY\)](https://creativecommons.org/licenses/by/4.0/). The use, distribution or
reproduction in other forums is permitted,
provided the original author(s) and the
copyright owner(s) are credited and that the
original publication in this journal is cited, in
accordance with accepted academic practice.
No use, distribution or reproduction is
permitted which does not comply with these
terms.

Comparative analysis of multimodal biomarkers for amyloid-beta positivity detection in Alzheimer's disease cohorts

Mostafa Mehdipour Ghazi^{1*}, Per Selnes^{2,3},
Santiago Timón-Reina², Sandra Tecalão², Silvia Ingala⁴,
Atle Bjørnerud^{5,6}, Bjørn-Eivind Kirsebom^{7,8}, Tormod Fladby^{2,3} and
Mads Nielsen¹

¹Department of Computer Science, Pioneer Centre for Artificial Intelligence, University of Copenhagen, Copenhagen, Denmark, ²Department of Neurology, Akershus University Hospital, Lørenskog, Norway, ³Institute of Clinical Medicine, Campus Ahus, University of Oslo, Oslo, Norway, ⁴Department of Radiology, Copenhagen University Hospital Rigshospitalet, Copenhagen, Denmark, ⁵Department of Physics, University of Oslo, Oslo, Norway, ⁶Unit for Computational Radiology and Artificial Intelligence, Oslo University Hospital, Oslo, Norway, ⁷Department of Neurology, University Hospital of North Norway, Tromsø, Norway, ⁸Department of Psychology, Faculty of Health Sciences, UiT The Arctic University of Norway, Tromsø, Norway

Introduction: Efforts to develop cost-effective approaches for detecting amyloid pathology in Alzheimer's disease (AD) have gained significant momentum with a focus on biomarker classification. Recent research has explored non-invasive and readily accessible biomarkers, including magnetic resonance imaging (MRI) biomarkers and some AD risk factors.

Methods: In this comprehensive study, we leveraged a diverse dataset, encompassing participants with varying cognitive statuses from multiple sources, including cohorts from the Alzheimer's Disease Neuroimaging Initiative (ADNI) and our in-house Dementia Disease Initiation (DDI) cohort. As brain amyloid plaques have been proposed as sufficient for AD diagnosis, our primary aim was to assess the effectiveness of multimodal biomarkers in identifying amyloid plaques, using deep machine learning methodologies.

Results: Our findings underscore the robustness of the utilized methods in detecting amyloid beta positivity across multiple cohorts. Additionally, we investigated the potential of demographic data to enhance MRI-based amyloid detection. Notably, the inclusion of demographic risk factors significantly improved our models' ability to detect amyloid-beta positivity, particularly in early-stage cases, exemplified by an average area under the ROC curve of 0.836 in the unimpaired DDI cohort.

Discussion: These promising, non-invasive, and cost-effective predictors of MRI biomarkers and demographic variables hold the potential for further refinement through considerations like APOE genotype and plasma markers.

KEYWORDS

Alzheimer's disease, amyloid-beta, magnetic resonance imaging, deep machine learning, biomarker classification

1 Introduction

Alzheimer's disease (AD) is a neurodegenerative condition that leads to cognitive dysfunction and eventual dementia (Gaugler et al., 2022). The initial event in AD pathophysiology is the extracellular deposition of amyloid beta (A β) plaques in the brain, which can occur up to 20 years before the onset of dementia (Karran and De Strooper, 2022). This extended prodementia phase offers a potential window for secondary prevention of AD dementia. However, defining the target population for such prevention strategies remains a lengthy, error-prone, and costly process (Scharre, 2019).

A β plaques are associated with longitudinal cognitive decline (Jack et al., 2013), and recently proposed guidelines (<https://aaic.alz.org/diagnostic-criteria.asp>) posit that they are sufficient to define AD. Research indicates that cognitive dysfunction in AD is closely linked to the deposition of intracellular tau neurofibrillary tangles (Braak and Braak, 1991). The combined impact of misfolded amyloid and tau proteins appears to trigger a cascade of events (Selkoe, 2001), that ultimately leads to dementia according to current disease models, albeit with varying timeframes. A β dysmetabolism leading to A β plaque deposition is followed by an extended pre-morbid and pre-dementia stage that may provide a window for intervention (Buchhave et al., 2012).

While amyloid and tau can be quantified through the analysis of cerebrospinal fluid (CSF) and positron emission tomography (PET) measures as well as plasma-based assays (Janelidze et al., 2016; Mattsson et al., 2016), defining neurodegeneration remains challenging. Current research criteria suggest that neurodegeneration can be measured using fluorodeoxyglucose (FDG) PET, magnetic resonance imaging (MRI), and CSF measurements (Schöll et al., 2019), but specific biomarkers and thresholds remain uncertain. These vague definitions, combined with the variable disease trajectories and clinical presentations, contribute to the heterogeneity of AD (Jack et al., 2013). Furthermore, the spatiotemporal relationships between AD biomarkers require further clarification, making the diagnostic and prognostic assessment of AD complex and necessitating a multimodal approach (Jack et al., 2018).

Several studies employing machine learning techniques to predict AD pathology have predominantly relied on single-cohort analysis with a limited number of multimodal biomarkers (Li et al., 2020; Tosun et al., 2021; Agostinho et al., 2022). Moreover, some investigations have strategically combined noninvasive and sensitive markers, including CSF measures and genetic data, with MRIs to underscore the effectiveness of integrating multimodal imaging and non-imaging markers for AD prediction, as demonstrated by Salvatore et al. (2015) and Moscoso et al. (2019). Despite these advancements, several limitations persist within the field in terms of data heterogeneity, constrained sample sizes, a limited number of cohorts, and the inherent challenges in harmonizing diverse datasets and biomarkers. Furthermore, the imperative for standardization across studies and validation in large, independent cohorts emerges as a critical necessity, ensuring that predictive models attain robust generalizability across varied populations and settings.

Considering the challenges inherent in AD pathology detection, our primary objective is the development of an artificial intelligence (AI) algorithm dedicated to predicting A β positivity and leveraging a comprehensive set of multimodal AD biomarkers in two distinct cohorts. Our study not only seeks to advance prediction model efficiency through novel machine learning methods but also holds the potential for cost reduction by leveraging noninvasive, readily available biomarkers. We rigorously validate this algorithm across multimodal biomarkers obtained from two independent non-demented cohorts, showcasing its robustness and applicability in diverse settings. The utilization of similar markers from these cohorts, matched based on analogous protocols and cutoffs, ensures compatibility and fairness in the acquired results. Additionally, our evaluation extends to the accuracy of models in predicting A β positivity by integrating noninvasive biomarkers, such as MRI measurements and demographic risk factors, with a specific emphasis on early-stage unimpaired cases.

2 Materials and methods

This section outlines the data sources, processing steps, biomarkers, and the experimental and analytical procedures employed for amyloid-beta positivity classification. A summary of the methods employed in the processing and analysis of the cohorts is provided in Figure 1. The tools and codes utilized for data preparation and analysis are available at <https://github.com/Mostafa-Ghazi/>.

2.1 Study participants

We used data from two distinct cohorts for the analysis. The first cohort was sourced from publicly available data (Petersen et al., 2010) via the Alzheimer's Disease Neuroimaging Initiative (ADNI) website. The second cohort comprised participants from an in-house dataset (Fladby et al., 2017) from the Dementia Disease Initiation (DDI) study conducted in Norway. Tables 1, 2 show demographic details of the utilized cohorts per clinical diagnostic group.

2.1.1 ADNI

The ADNI was launched in 2003 as a public-private partnership, led by principal investigator Michael W. Weiner, MD. The primary goal of ADNI has been to test whether serial MRI, PET, other biological markers, and clinical and neuropsychological assessment can be combined to measure the progression of mild cognitive impairment (MCI) and early Alzheimer's disease. We included all participants from the ADNI-MERGE (1/GO/2/3) cohorts with available clinical dementia rating (CDR) values and A β status. This led to a dataset comprising 1,218 unimpaired and 1,293 impaired patients with missing modality biomarkers from the ADNI cohort. Refer to Table 1 for demographic details.

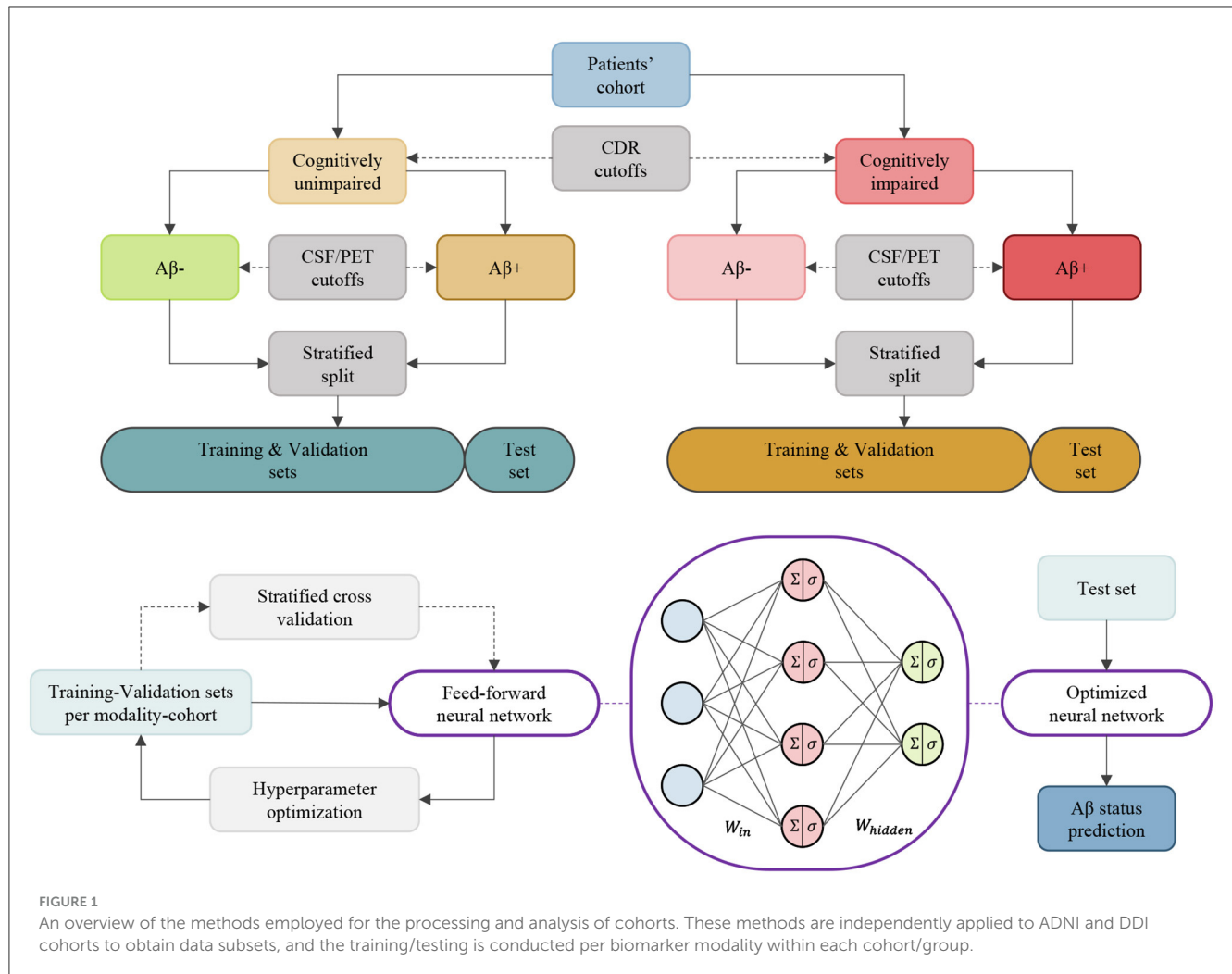


TABLE 1 Demographics of the ADNI cohorts per clinical diagnostic group.

	Cognitively unimpaired		Cognitively impaired	
	Aβ–	Aβ+	Aβ–	Aβ+
# Subjects (male vs. female)	186/202	96/147	184/137	254/218
# Visits	795	423	576	717
APOE allele ($\epsilon - / \epsilon +$ ratio)	3.97	1.23	3.94	0.62
Age (years)	74.61 ± 7.26	77.15 ± 7.00	73.16 ± 8.65	75.38 ± 7.39
Education (years)	16.74 ± 2.50	16.42 ± 2.61	16.25 ± 2.66	16.03 ± 2.74
MMSE score	29.08 ± 1.20	28.80 ± 1.38	28.23 ± 1.98	26.84 ± 2.63

2.1.2 DDI

The multi-site DDI cohort study comprised at-risk and clinical cases with subjective cognitive decline (SCD) (Jessen et al., 2014) and MCI (Albert et al., 2011) who had standardized MRI and CSF measurements (Fladby et al., 2017; Siafarikas et al., 2021). In addition, healthy controls (HC) were included from spouses of patients and from patients who completed lumbar punctures in connection with orthopedic surgery. For both cases and controls, MRI scans, neuropsychological assessments, and samples of plasma and CSF were collected within 3 months of

inclusion. Ethical approval for the study was obtained from the Regional Committees for Medical and Health Research Ethics (REK), ensuring compliance with ethical standards. All participants provided written informed consent, and all research procedures adhered to the relevant REK guidelines and the principles outlined in the Declaration of Helsinki. We included all participants from the DDI cohorts with available CDR values and Aβ status. This led to a dataset comprising 441 unimpaired and 413 impaired patients with missing modality biomarkers from the DDI cohort. Refer to Table 2 for demographic details.

TABLE 2 Demographics of the DDI cohorts per clinical diagnostic group.

	Cognitively unimpaired		Cognitively impaired	
	A β –	A β +	A β –	A β +
# Subjects (male vs. female)	113/137	32/53	83/73	74/74
# Visits	333	108	222	191
APOE allele (ϵ –/ ϵ + ratio)	1.94	0.64	2.32	0.42
Age (years)	62.30 \pm 9.53	68.21 \pm 7.10	65.38 \pm 9.06	70.47 \pm 7.93
Education (years)	13.95 \pm 2.88	14.18 \pm 3.13	13.68 \pm 3.31	13.23 \pm 3.50
MMSE score	28.78 \pm 1.76	28.73 \pm 1.55	28.62 \pm 1.73	27.49 \pm 2.72

2.2 Study biomarkers

We used multimodal biomarkers to study A β positivity of different cohorts. These markers were selected from demographic risk factors, cognitive scores, and CSF and imaging (MRI/PET) measurements. Figures 2, 3 illustrate the distribution of some selected key multimodal AD biomarkers utilized in this study from the two datasets.

2.2.1 Risk factors

To capture and assess risk factors, we selected the demographic variables of age, sex, and years of education as key determinants within both the ADNI and DDI cohorts.

2.2.2 Cognitive scores

In both the ADNI and DDI cohorts, we employed scores from the Mini-Mental State Examination (MMSE) and the Clinical Dementia Rating-Sum of Boxes (CDR-SB). Furthermore, we utilized the Alzheimer's Disease Assessment Scale Cognitive (ADAS-Cog) with 13 items from the ADNI dataset and the learning subscale of the Consortium to Establish a Registry for Alzheimer's Disease (CERAD-Learning) from the DDI dataset. The classification of individuals into cognitively unimpaired (CU) or impaired (CI) categories was based on CDR values, where a CDR score of 0 indicated unimpaired status, and a score of 0.5 signified impairment (Morris et al., 2001; Aisen et al., 2010).

2.2.3 CSF and PET measures

A β 42, A β 40, phosphorylated tau (p-tau181), total tau (t-tau), Neurogranin (Ng), and β -site amyloid-precursor-protein cleaving enzyme 1 (BACE1) were partially quantified in the CSF samples collected from both the ADNI and DDI cohorts. Pathological A β levels in the ADNI dataset were determined by applying a threshold of 1.11 to the radiotracer florbetapir (18F-AV-45) in PET scans without using CSF biomarkers, as previously validated by Royse et al. (2021). More specifically, we categorized patients with 18F-AV-45 values \geq 1.11 into the A β + group, while those with values below this threshold were assigned to the A β – group. In the DDI dataset, we established A β 42/40 ratio cutoffs with a range of 0.077, derived from receiver operating curve (ROC) analysis using visual read results of Flutemetamol (18F-Flut) PET scans as the standard

reference (Siafarikas et al., 2021). A β measurements were excluded from predictor variables in the model, as they were partially used for status definition in DDI and represent the same features as measured with PET in ADNI. Note that we achieved an area under the ROC curve of 0.98 when fitting A β 42 values using decision trees for binary 18F-AV-45 classification. Moreover, since there were not enough ADNI samples with available Ng and BACE1 measurements, we only used p-tau181 and t-tau variables for the classification purpose in ADNI.

2.2.4 MRI measures

MRI scans were obtained on multi-vendor systems including Siemens, Philips, and GE, at field strengths of 1.5 and 3 T. The T1-weighted images were used for volumetric analysis with slice thicknesses from 1 to 2 mm, while diffusion-weighted imaging (DWI) series were used for diffusion tensor-based analysis.

T1-weighted volumetric assessments were conducted using distinct segmentation tools: FreeSurfer (Fischl et al., 2002) in the ADNI cohort and the FAST-AID Brain (Mehdipour Ghazi and Nielsen, 2022) in the DDI cohort. Regional volumes were computed based on the segmentation results obtained from T1-weighted brain MRI scans. Subsequently, these estimated volumes were adjusted for the total intracranial volume (ICV). In the ADNI dataset, the analysis encompassed 6 brain regions, comprising the ventricles, hippocampus, entorhinal cortex, fusiform gyrus, middle temporal gyrus, and the whole brain. Conversely, the DDI cohort examined a more extensive set of 68 regions, encompassing both left and right compartments of the 132 segmented areas combined.

DWI scans underwent rigorous analysis using the FSL tool (Smith et al., 2004). To ensure data accuracy, corrections were applied to mitigate Eddy-current distortion and head motion, taking into consideration the available b0 scan. Subsequently, a diffusion tensor was modeled at every voxel within the brain, utilizing the FSL fit function on the corrected DWI scans. Scalar anisotropy and diffusivity maps were derived from the eigenvalues of the diffusion tensor, yielding fractional anisotropy (FA), axial diffusivity (AD), radial diffusivity (RD), and mean diffusivity (MD). To unveil spatial patterns of interest, a voxel-wise statistical analysis of the DTI maps was executed via the TBSS function (Smith et al., 2006). The corrected FA images were then registered to the white-matter tractography atlas sourced from Johns Hopkins University (JHU) (Hua et al., 2008). This process resulted in the calculation

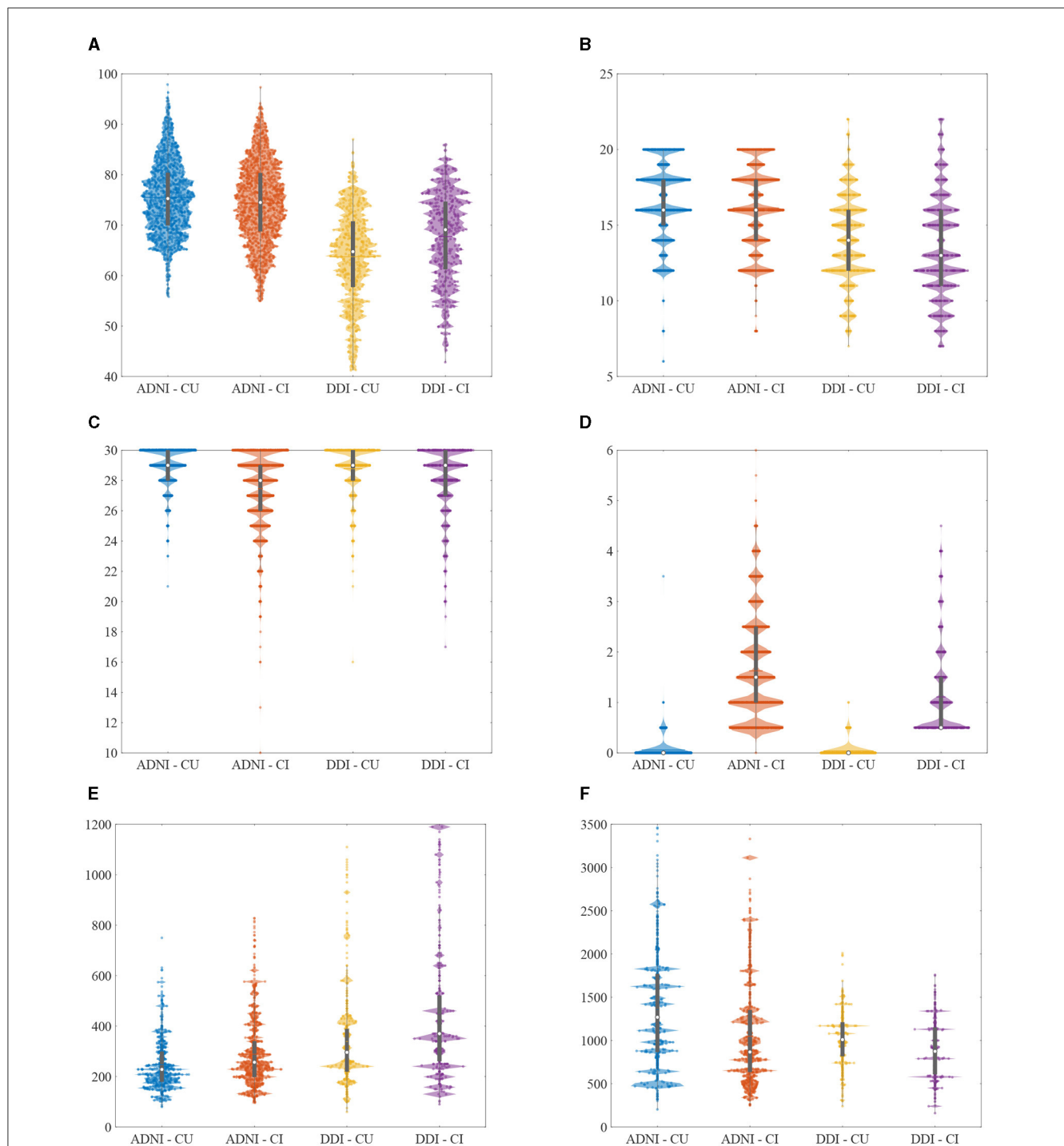


FIGURE 2
Violin plots of the selected non-imaging AD biomarkers utilized in this study from different cohorts. Note that clipped values of $A\beta_{42}$ ($>1,700$ or <200) were replaced with the recalculated results. **(A)** Age (years). **(B)** Education (years). **(C)** MMSE (scores). **(D)** CDR-SB (scores). **(E)** T-tau (pg/mL). **(F)** $A\beta_{42}$ (pg/mL).

of 20 and 57 regions of interest (ROIs) for each anisotropy and diffusivity feature within the DDI and ADNI datasets, respectively.

2.3 Statistical analysis

The statistical analysis involved the utilization of appropriate tests based on variable type and group comparisons. For continuous

variables within both the impaired and unimpaired cohorts, the nonparametric Wilcoxon rank-sum test was employed to assess statistical differences between the two groups ($A\beta_{42}$). Categorical variables, on the other hand, were subject to Fisher's exact test when dealing with binary outcomes, and the Chi-squares test when analyzing groups with nonbinary values. A significance threshold of $p < 0.05$ was employed to guide the determination of hypothesis test outcomes.

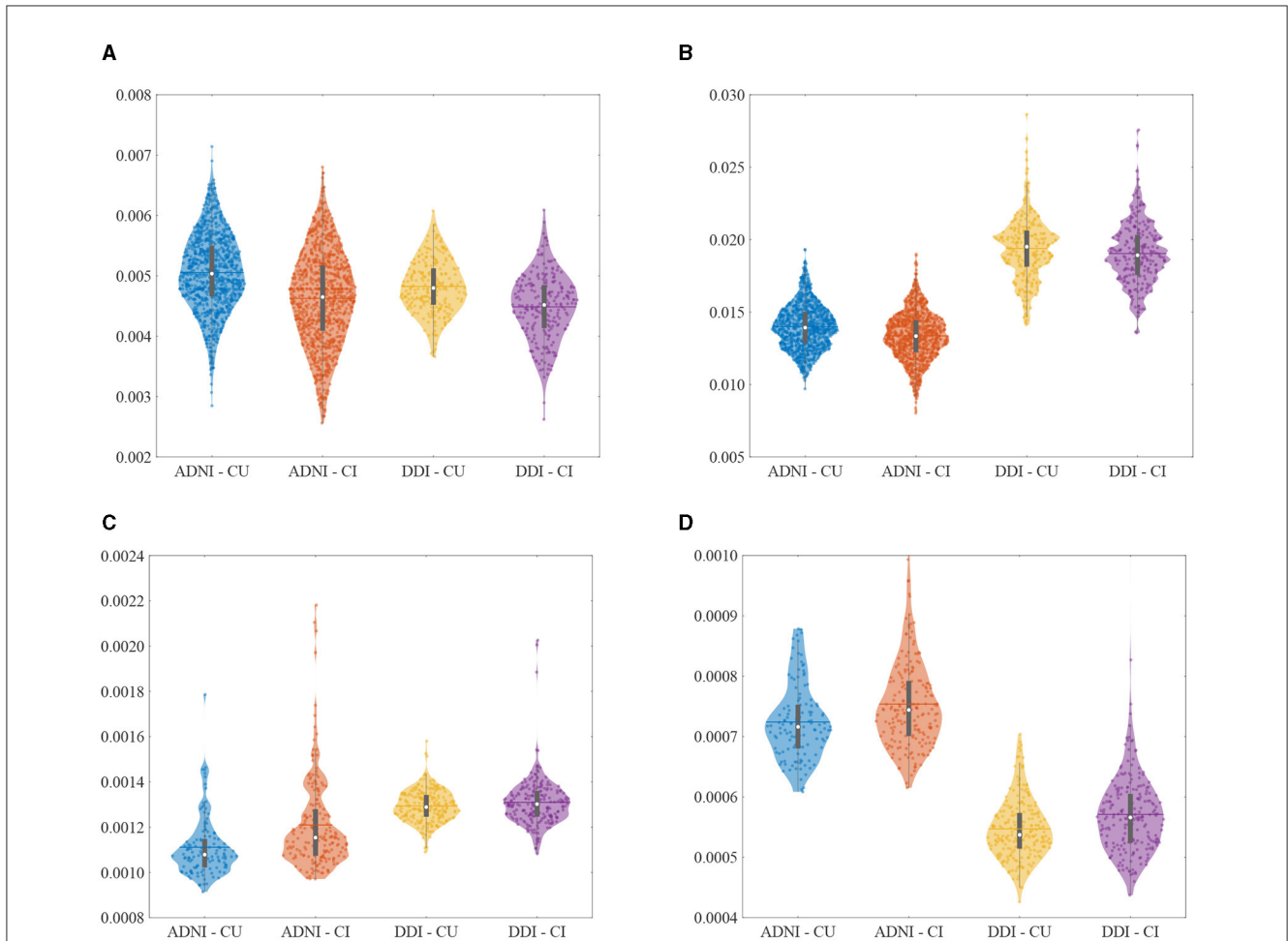


FIGURE 3 Violin plots of the selected imaging AD biomarkers utilized in this study from different cohorts. **(A)** Hippocampus volume (normalized). **(B)** Middle temporal gyrus (normalized). **(C)** Uncinate fasciculus (AD). **(D)** Inf fronto-occipital fasciculus (RD).

TABLE 3 Aβ status classification results (five-fold mean ± SD) for the unimpaired group of the test ADNI.

Biomarker	# Samples	AUC	Accuracy	Sensitivity	Specificity	Precision
Cognitive	243	0.603 ± 0.004	0.597 ± 0.005	0.500 ± 0.017	0.648 ± 0.006	0.429 ± 0.007
CSF	114	0.862 ± 0.007	0.802 ± 0.008	0.784 ± 0.019	0.810 ± 0.015	0.666 ± 0.015
T1-MRI	187	0.651 ± 0.012	0.634 ± 0.008	0.512 ± 0.058	0.694 ± 0.028	0.447 ± 0.012
Diffusion-MRI	24	0.825 ± 0.049	0.775 ± 0.037	0.514 ± 0.163	0.882 ± 0.042	0.644 ± 0.057
T1-MRI and risk	187	0.720 ± 0.013	0.726 ± 0.010	0.489 ± 0.058	0.841 ± 0.022	0.599 ± 0.018

TABLE 4 Aβ status classification results (five-fold mean ± SD) for the impaired group of the test ADNI.

Biomarker	# Samples	AUC	Accuracy	Sensitivity	Specificity	Precision
Cognitive	258	0.760 ± 0.001	0.709 ± 0.000	0.632 ± 0.004	0.805 ± 0.005	0.801 ± 0.003
CSF	155	0.925 ± 0.003	0.849 ± 0.013	0.873 ± 0.024	0.816 ± 0.007	0.871 ± 0.004
T1-MRI	194	0.753 ± 0.002	0.697 ± 0.004	0.737 ± 0.011	0.649 ± 0.017	0.713 ± 0.008
Diffusion-MRI	37	0.828 ± 0.027	0.735 ± 0.048	0.760 ± 0.022	0.706 ± 0.083	0.755 ± 0.059
T1-MRI and risk	194	0.862 ± 0.003	0.777 ± 0.024	0.792 ± 0.021	0.760 ± 0.043	0.796 ± 0.030

TABLE 5 A β status classification results (five-fold mean \pm SD) for the unimpaired group of the test DDI.

Biomarker	# Samples	AUC	Accuracy	Sensitivity	Specificity	Precision
Cognitive	88	0.590 \pm 0.008	0.602 \pm 0.043	0.514 \pm 0.052	0.630 \pm 0.070	0.306 \pm 0.025
CSF	80	0.843 \pm 0.016	0.858 \pm 0.019	0.670 \pm 0.027	0.920 \pm 0.022	0.739 \pm 0.057
T1-MRI	48	0.674 \pm 0.010	0.671 \pm 0.040	0.415 \pm 0.042	0.766 \pm 0.055	0.402 \pm 0.060
Diffusion-MRI	44	0.753 \pm 0.008	0.809 \pm 0.026	0.517 \pm 0.109	0.919 \pm 0.036	0.716 \pm 0.079
T1-MRI and risk	48	0.836 \pm 0.015	0.746 \pm 0.040	0.569 \pm 0.129	0.811 \pm 0.033	0.526 \pm 0.063

TABLE 6 A β status classification results (five-fold mean \pm SD) for the impaired group of the test DDI.

Biomarker	# Samples	AUC	Accuracy	Sensitivity	Specificity	Precision
Cognitive	82	0.732 \pm 0.007	0.654 \pm 0.014	0.658 \pm 0.065	0.650 \pm 0.061	0.621 \pm 0.026
CSF	69	0.910 \pm 0.003	0.829 \pm 0.019	0.820 \pm 0.018	0.840 \pm 0.029	0.794 \pm 0.030
T1-MRI	44	0.785 \pm 0.029	0.736 \pm 0.057	0.756 \pm 0.101	0.723 \pm 0.032	0.652 \pm 0.052
Diffusion-MRI	43	0.682 \pm 0.012	0.637 \pm 0.027	0.553 \pm 0.067	0.692 \pm 0.000	0.539 \pm 0.030
T1-MRI and risk	44	0.805 \pm 0.044	0.723 \pm 0.059	0.678 \pm 0.107	0.754 \pm 0.044	0.654 \pm 0.062

2.4 Amyloid-beta status prediction

Our approach for A β \pm classification involved the utilization of feedforward artificial neural networks comprising two fully connected layers with learnable parameters and nonlinear activation functions. These networks were employed to predict the A β status by leveraging multivariate biomarkers from each modality, both individually and in combination. These networks underwent supervised training, during which they learned to encode high-dimensional input data, abstracting latent variables while disregarding insignificant information and minimizing classification errors through an output layer.

To optimize the network's performance and ensure robustness, we conducted a rigorous training and inference process. We randomly partitioned each of the two datasets into training (80%) and testing (20%) subsets using a stratified approach. We applied a five-fold stratified cross-validation and testing procedure to the training and test data to tune the network's hyperparameters, allowing at most 1,000 iterations, and to assess the generalization capability.

We assessed the performance of our prediction models by employing key metrics including total accuracy, the area under the ROC curve (AUC), precision, recall (sensitivity), and specificity. These metrics were consistently evaluated across various cross-validation folds applied to the test sets. This approach allows for a comprehensive interpretation of results, effectively addressing concerns related to data size, biases, and classification errors of any kind.

3 Results

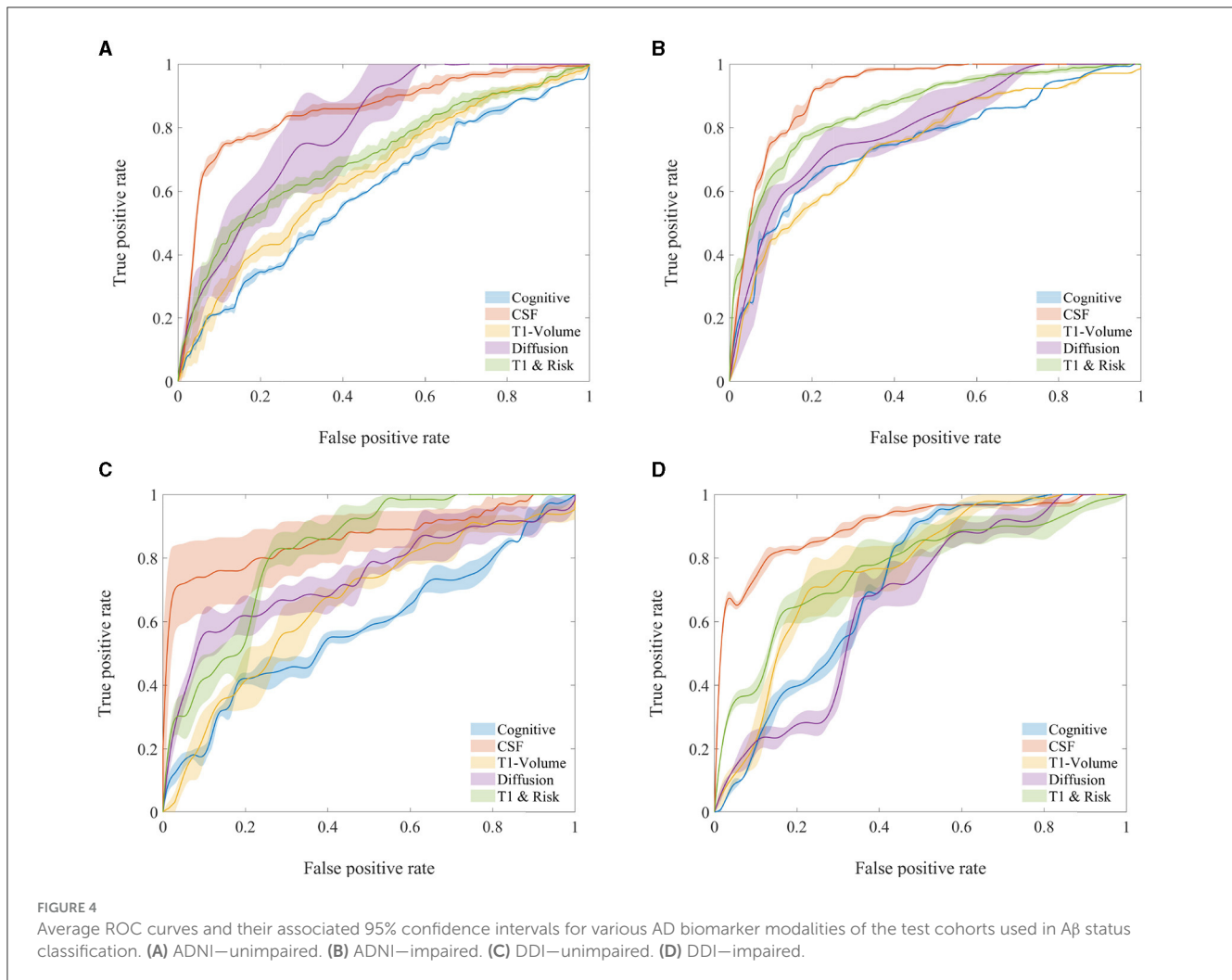
In the ADNI cohorts considering both impaired and unimpaired individuals, several key variables exhibited statistically significant differences between the A β \pm groups. These variables included age, ADAS-Cog, MMSE, p-tau, t-tau, A β 42, as well as the

volumetric measurements of ventricles, hippocampus, whole brain, and 47 regional diffusion parameters. Similarly, within the DDI cohorts comprising both impaired and unimpaired individuals, the A β \pm groups demonstrated notable disparities in various variables. Specifically, age, CERAD-Learning, p-tau, t-tau, BACE1, Ng, volumes of seven distinct brain regions, and two regional diffusion measures displayed statistically significant differences between the two A β groups. Figure 5 depicts a visual representation of the statistical analysis conducted on the ADNI biomarkers.

Within the impaired ADNI cohort, significant differences between the A β \pm groups were observed in CDR-SB, volumetric measurements of the entorhinal, fusiform, and middle temporal gyrus, as well as seven regional diffusion metrics. Conversely, in the unimpaired ADNI cohort, distinctions emerged in terms of sex, years of education, and 136 regional diffusion measures. Besides, in the impaired DDI cohort, A β \pm group disparities were evident in CDR-SB and MMSE scores, volumes spanning 33 distinct brain regions, and two regional diffusion metrics. However, in the unimpaired DDI cohort, significant differences were only noted in terms of sex and a regional diffusion measure. Figure 6 presents a visual representation of the statistical analysis conducted on the DDI biomarkers.

Tables 3–6 provide a comprehensive summary of the A β status classification outcomes obtained from the test sets within the ADNI and DDI cohorts, covering both the impaired and unimpaired groups. The results suggest that CSF measures exhibit the highest accuracy, with imaging markers and cognitive scores following behind. Additionally, the minimal fluctuations observed around the average accuracies show the robustness of the models across various cross-validation folds. Furthermore, the congruence in results between the ADNI and DDI cohorts underscores the generalizability of these models.

To complement the result interpretation, we have additionally provided visual representations of the ROC curves in Figure 4 for all cohorts within the utilized test sets. The observed variability in the diffusion-MRI measurements can be attributed to the limited



availability of data points in this specific modality. Furthermore, the lower and fluctuating accuracy of CSF measurements in the unimpaired DDI cohort, compared to alternative modalities and cohorts, may be attributed to slight differences in the CSF measurement protocols between DDI and ADNI, potentially influencing the detection of A β positivity in the unimpaired groups. It is also worth noting that the higher accuracies achieved by the T1-MRI measures in the DDI cohorts can be primarily attributed to the utilization of a larger set of robust regional volumes obtained through FAST-AID Brain.

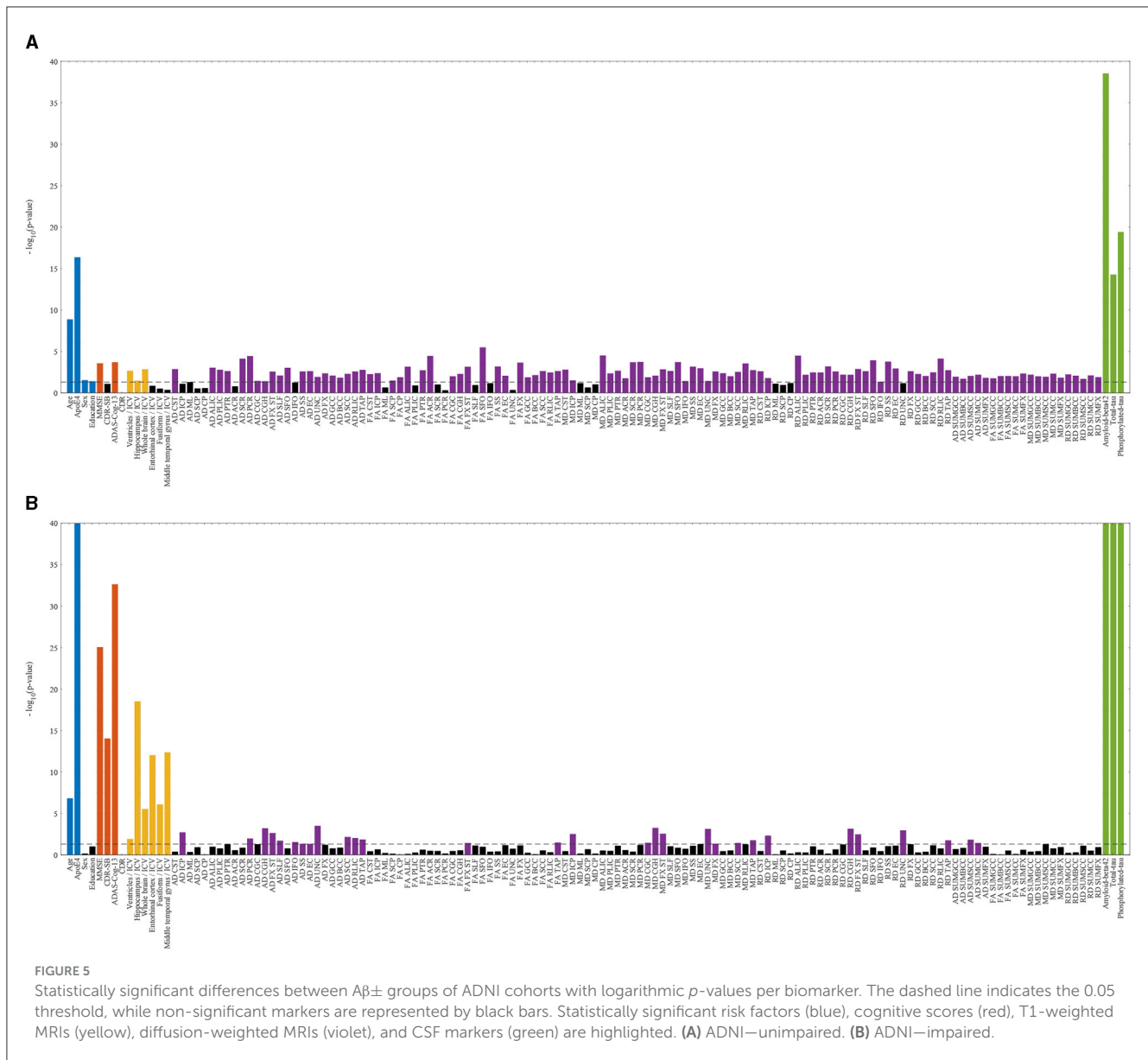
4 Discussion

This study leveraged two distinct cohorts, ADNI and DDI, characterized by nearly the same sets of biomarkers, ensuring a fair and comprehensive analysis. When comparing the clinical-demographic differences between the ADNI and DDI cohorts, patients in the ADNI cohort tend to be older than those in the DDI cohort, yet they possess a higher number of education years. Additionally, the ADNI cohort exhibits a lower percentage of cases with APOE+ alleles compared to the DDI cohort. The distribution

of subjects by sex is nearly equivalent in both ADNI and DDI, with a higher proportion of females in the unimpaired cohort and a greater prevalence of males in the impaired cohort.

The prediction results obtained in this study reveal consistent accuracies across both the ADNI and DDI cohorts for A β status classification using deep learning models. Notably, CSF markers yielded the highest accuracy, followed by imaging biomarkers and cognitive scores. This pattern aligns with previous research, including the hypothetical model proposed by Jack et al. (2010) and the latest studies on multimodal biomarkers of AD (Tosun et al., 2021). The consistent findings underscore the robustness and generalizability of our models in achieving these accuracies.

The high AUCs obtained using non-amyloid CSF variables for the unimpaired and impaired groups implicate amyloid-related neurodegeneration both at early stages and during AD progression (Kirsebom et al., 2018, 2022). Besides, our classification results were more favorable in the impaired cohorts, attributed to the presence of pronounced biomarker changes and cognitive impairment developments in these groups. This trend mirrors earlier findings in the literature (Tosun et al., 2021), highlighting the relative challenges



of $A\beta$ status classification within the cognitively normal populations.

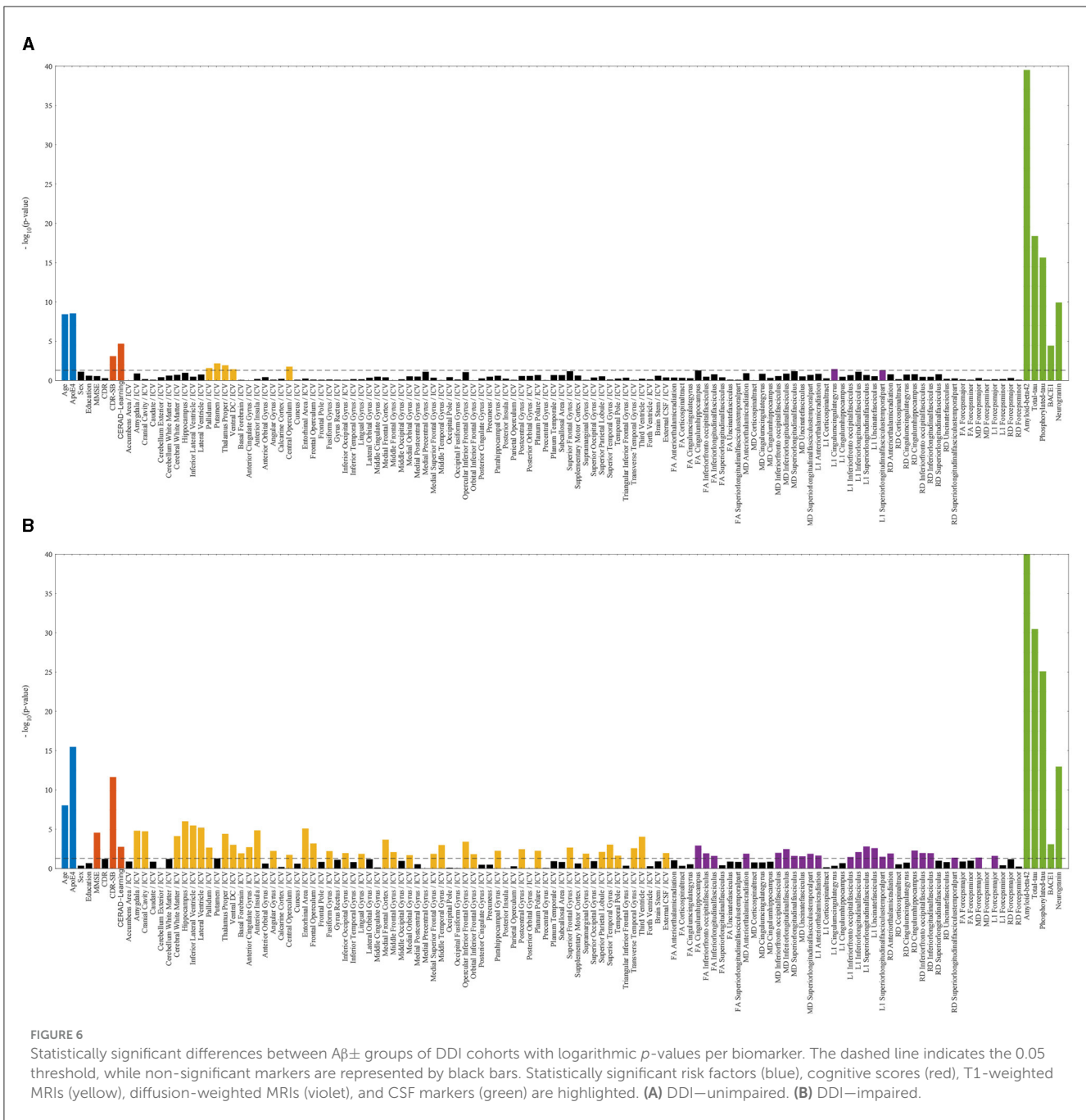
The high AUCs for diffusion-weighted and T1-weighted MRIs are in accordance with early changes in diffusivity measures and later neurodegenerative changes (Selnes et al., 2013). In the ADNI cohorts, the limited size of diffusion-weighted MRI data precludes a definitive conclusion regarding their performance compared to T1-weighted MRIs. In the DDI cohort, diffusion-weighted MRI markers exhibit higher accuracy in predicting $A\beta$ positivity among early AD patients within the unimpaired cohort. Still, the observed discrepancy in results is greater compared to T1-weighted MRIs.

In general, cognitive markers exhibit lower predictive power for AD compared to imaging and CSF markers, aligning with findings in the existing literature discussed in various hypothetical, statistical, and learning models (Jack et al., 2013; Mehdipour Ghazi et al., 2019, 2021). However, it is noteworthy that certain cognitive or neuropsychological biomarkers, such

as auditory-verbal assessments, have demonstrated substantial efficacy in detecting AD in the early stages (Zandifar et al., 2020; Mehdipour Ghazi et al., 2021).

The results from the statistical analyses presented in Figures 5, 6 reveal statistically significant differences in some demographic risk factors and all CSF measures between $A\beta\pm$ groups across all cases. Additionally, as cohorts transition to impairment, various biomarkers, including cognitive scores and MRI measurements, demonstrate significance. Notably, T1-weighted MRIs are particularly emphasized in the impaired DDI cohort, benefiting from a detailed regional analysis provided by FAST-AID Brain. Conversely, diffusion-weighted MRIs exhibit prominence in the unimpaired ADNI cohort, possibly attributed to the utilization of a more extensive set of regional markers and a smaller dataset from ADNI.

Furthermore, the combination of MRI measurements with demographic risk factors demonstrated an enhancement in



classification performance across different scenarios. The literature has previously demonstrated the enhanced accuracy achieved through the concatenation of MRI measurements with other risk factors (Ten Kate et al., 2018; Tosun et al., 2021). Particularly intriguing is the observation that this improvement was more pronounced in the unimpaired cohorts. This outcome bears significant implications for early AD detection using noninvasive biomarkers, where early and accurate identification within this subset of individuals holds particular importance.

Finally, the utilized noninvasive and cost-effective predictors involving MRI biomarkers and demographic variables show promise for refinement through additional considerations, such as the APOE genotype and plasma markers. However, it is

essential to acknowledge that utilizing the APOE genotype introduces challenges, mainly rooted in ethical considerations, privacy concerns, and the sensitivity of genetic information. On the contrary, plasma markers pose challenges due to their limited establishment in AD research, potentially hindered by a lack of substantial representation in large cohorts alongside other markers for comprehensive analysis.

Data availability statement

The data analyzed in this study is subject to the following licenses/restrictions. The public ADNI datasets utilized in this

study are accessible via <https://adni.loni.usc.edu/data-samples/access-data/>. However, the in-house DDI datasets used in this article are not readily available due to ethical and patient privacy restrictions. Requests to access these datasets should be directed at: TF (tormod.fladby@medisin.uio.no).

Ethics statement

Ethical approval was not required for the study involving humans in accordance with the local legislation and institutional requirements. Written informed consent to participate in this study was not required from the participants or the participants' legal guardians/next of kin in accordance with the national legislation and the institutional requirements.

Author contributions

MM: Conceptualization, Formal analysis, Investigation, Methodology, Software, Validation, Visualization, Writing—original draft. PS: Conceptualization, Investigation, Project administration, Supervision, Validation, Writing—review & editing. ST-R: Data curation, Resources, Writing—review & editing. ST: Resources, Writing—review & editing. SI: Writing—review & editing. AB: Writing—review & editing. B-EK: Resources, Writing—review & editing. TF: Funding acquisition, Project administration, Supervision, Writing—review & editing. MN: Funding acquisition, Project administration, Supervision, Writing—review & editing.

Funding

The author(s) declare financial support was received for the research, authorship, and/or publication of this article. This project has received funding from the European Union's Horizon 2020 research and innovation programme under the Marie Skłodowska-Curie grant agreement nos. 643417, 681043, and 825664, VELUX FONDEN and Innovation Fund Denmark under grant number 9084-00018B, Pioneer Centre for AI, Danish National Research Foundation, grant number P1, and Research Council of Norway under project number 311993 (JPND/PMI-AD).

Acknowledgments

Data collection and sharing for this project was funded by the Alzheimer's Disease Neuroimaging Initiative (ADNI) (National

Institutes of Health Grant U01 AG024904) and DOD ADNI (Department of Defense award number W81XWH-12-2-0012). ADNI was funded by the National Institute on Aging, the National Institute of Biomedical Imaging and Bioengineering, and through generous contributions from the following: AbbVie, Alzheimer's Association; Alzheimer's Drug Discovery Foundation; Araclon Biotech; BioClinica, Inc.; Biogen; Bristol-Myers Squibb Company; CereSpir, Inc.; Cogstate; Eisai Inc.; Elan Pharmaceuticals, Inc.; Eli Lilly and Company; EuroImmun; F. Hoffmann-La Roche Ltd. and its affiliated company Genentech, Inc.; Fujirebio; GE Healthcare; IXICO Ltd.; Janssen Alzheimer Immunotherapy Research & Development, LLC.; Johnson & Johnson Pharmaceutical Research & Development LLC.; Lumosity; Lundbeck; Merck & Co., Inc.; Meso Scale Diagnostics, LLC.; NeuroRx Research; Neurotrack Technologies; Novartis Pharmaceuticals Corporation; Pfizer Inc.; Piramal Imaging; Servier; Takeda Pharmaceutical Company; and Transition Therapeutics. The Canadian Institutes of Health Research is providing funds to support ADNI clinical sites in Canada. Private sector contributions are facilitated by the Foundation for the National Institutes of Health (www.fnih.org). The grantee organization is the Northern California Institute for Research and Education, and the study is coordinated by the Alzheimer's Therapeutic Research Institute at the University of Southern California. ADNI data are disseminated by the Laboratory for Neuro Imaging at the University of Southern California.

Conflict of interest

The authors declare that the research was conducted in the absence of any commercial or financial relationships that could be construed as a potential conflict of interest.

The author(s) declared that they were an editorial board member of Frontiers, at the time of submission. This had no impact on the peer review process and the final decision.

Publisher's note

All claims expressed in this article are solely those of the authors and do not necessarily represent those of their affiliated organizations, or those of the publisher, the editors and the reviewers. Any product that may be evaluated in this article, or claim that may be made by its manufacturer, is not guaranteed or endorsed by the publisher.

References

- Agostinho, D., Caramelo, F., Moreira, A. P., Santana, I., Abrunhosa, A., Castelo-Branco, M., et al. (2022). Combined structural MR and diffusion tensor imaging classify the presence of Alzheimer's disease with the same performance as MR combined with amyloid positron emission tomography: a data integration approach. *Front. Neurosci.* 15:638175. doi: 10.3389/fnins.2021.638175
- Aisen, P. S., Petersen, R. C., Donohue, M. C., Gamst, A., Raman, R., Thomas, R. G., et al. (2010). Clinical core of the Alzheimer's disease neuroimaging initiative: progress and plans. *Alzheimers Dement.* 6, 239–246. doi: 10.1016/j.jalz.2010.03.006
- Albert, M. S., DeKosky, S. T., Dickson, D., Dubois, B., Feldman, H. H., Fox, N. C., et al. (2011). The diagnosis of mild cognitive impairment due to Alzheimer's disease:

- recommendations from the National Institute on Aging-Alzheimer's Association workgroups on diagnostic guidelines for Alzheimer's disease. *Alzheimers Dement.* 7, 270–279. doi: 10.1016/j.jalz.2011.03.008
- Braak, H., and Braak, E. (1991). Neuropathological staging of Alzheimer-related changes. *Acta Neuropathol.* 82, 239–259. doi: 10.1007/BF00308809
- Buchhave, P., Minthon, L., Zetterberg, H., Wallin, Å. K., Blennow, K., and Hansson, O. (2012). Cerebrospinal fluid levels of β -amyloid 1-42, but not of tau, are fully changed already 5 to 10 years before the onset of Alzheimer dementia. *Arch. Gen. Psychiatry* 69, 98–106. doi: 10.1001/archgenpsychiatry.2011.155
- Fischl, B., Salat, D. H., Busa, E., Albert, M., Dieterich, M., Haselgrove, C., et al. (2002). Whole brain segmentation: automated labeling of neuroanatomical structures in the human brain. *Neuron* 33, 341–355. doi: 10.1016/S0896-6273(02)00569-X
- Fladby, T., Pålhaugen, L., Selnes, P., Bråthen, G., Hessen, E., Almdahl, I. S., et al. (2017). Detecting at-risk Alzheimer's disease cases. *J. Alzheimers Dis.* 60, 97–105. doi: 10.3233/JAD-170231
- Gaugler, J., James, B., Johnson, T., Reimer, J., Solis, M., Weuve, J., et al. (2022). 2022 Alzheimer's disease facts and figures. *Alzheimers Dement.* 18, 700–789. doi: 10.1002/alz.12638
- Hua, K., Zhang, J., Wakana, S., Jiang, H., Li, X., Reich, D. S., et al. (2008). Tract probability maps in stereotaxic spaces: analyses of white matter anatomy and tract-specific quantification. *Neuroimage* 39, 336–347. doi: 10.1016/j.neuroimage.2007.07.053
- Jack Jr, C. R., Bennett, D. A., Blennow, K., Carrillo, M. C., Dunn, B., Haeblerlein, S. B., et al. (2018). NIA-AA research framework: toward a biological definition of Alzheimer's disease. *Alzheimers Dement.* 14, 535–562. doi: 10.1016/j.jalz.2018.02.018
- Jack Jr, C. R., Knopman, D. S., Jagust, W. J., Petersen, R. C., Weiner, M. W., Aisen, P. S., et al. (2013). Update on hypothetical model of Alzheimer's disease biomarkers. *Lancet Neurol.* 12:207.
- Jack, C. R., Knopman, D. S., Jagust, W. J., Petersen, R. C., Weiner, M. W., Aisen, P. S., et al. (2013). Tracking pathological processes in Alzheimer's disease: an updated hypothetical model of dynamic biomarkers. *Lancet Neurol.* 12, 207–216. doi: 10.1016/S1474-4422(12)70291-0
- Jack, C. R., Knopman, D. S., Jagust, W. J., Shaw, L. M., Aisen, P. S., Weiner, M. W., et al. (2010). Hypothetical model of dynamic biomarkers of the Alzheimer's pathological cascade. *Lancet Neurol.* 9, 119–128.
- Janelidze, S., Stomrud, E., Palmqvist, S., Zetterberg, H., Van Westen, D., Jeromin, A., et al. (2016). Plasma β -amyloid in Alzheimer's disease and vascular disease. *Sci. Rep.* 6:26801. doi: 10.1038/srep26801
- Jessen, F., Amariglio, R. E., Van Boxtel, M., Breteler, M., Ceccaldi, M., Chételat, G., et al. (2014). A conceptual framework for research on subjective cognitive decline in preclinical Alzheimer's disease. *Alzheimers Dement.* 10, 844–852. doi: 10.1016/j.jalz.2014.01.001
- Karran, E., and De Strooper, B. (2022). The amyloid hypothesis in Alzheimer's disease: new insights from new therapeutics. *Nat. Rev. Drug Discov.* 21, 306–318. doi: 10.1038/s41573-022-00391-w
- Kirsebom, B.-E., Nordengen, K., Selnes, P., Torsetnes, S. B., Gisladóttir, B., Brix, B., et al. (2018). Cerebrospinal fluid neurogranin/ β -site APP-cleaving enzyme 1 predicts cognitive decline in preclinical Alzheimer's disease. *Alzheimers Dement.* 4, 617–627. doi: 10.1016/j.trci.2018.10.003
- Kirsebom, B. E., Richter, G., Nordengen, K., Aarsland, D., Bråthen, G., Tijms, B. M., et al. (2022). Stable cerebrospinal fluid neurogranin and β -site amyloid precursor protein cleaving enzyme 1 levels differentiate pre-dementia Alzheimer's disease patients. *Brain Commun.* 4:fcac244. doi: 10.1093/braincomms/fcac244
- Li, B., Zhang, M., Riphagen, J., Yochim, K. M., Li, B., Liu, J., et al. (2020). Prediction of clinical and biomarker conformed Alzheimer's disease and mild cognitive impairment from multi-feature brain structural MRI using age-correction from a large independent lifespan sample. *Neuroimage Clin.* 28:102387. doi: 10.1016/j.nicl.2020.10.2387
- Mattsson, N., Zetterberg, H., Janelidze, S., Insel, P. S., Andreasson, U., Stomrud, E., et al. (2016). Plasma tau in Alzheimer disease. *Neurology* 87, 1827–1835. doi: 10.1212/WNL.0000000000003246
- Mehdipour Ghazi, M., and Nielsen, M. (2022). FAST-AID brain: fast and accurate segmentation tool using artificial intelligence developed for brain. *arXiv*. [Preprint]. doi: 10.48550/arXiv.2208.14360
- Mehdipour Ghazi, M., Nielsen, M., Pai, A., Cardoso, M. J., Modat, M., Ourselin, S., et al. (2019). Training recurrent neural networks robust to incomplete data: application to Alzheimer's disease progression modeling. *Med. Image Anal.* 53, 39–46. doi: 10.1016/j.media.2019.01.004
- Mehdipour Ghazi, M., Nielsen, M., Pai, A., Modat, M., Cardoso, M. J., et al. (2021). Robust parametric modeling of Alzheimer's disease progression. *Neuroimage* 225:117460. doi: 10.1016/j.neuroimage.2020.117460
- Morris, J. C., Storandt, M., Miller, J. P., McKeel, D. W., Price, J. L., Rubin, E. H., et al. (2001). Mild cognitive impairment represents early-stage Alzheimer disease. *Arch. Neurol.* 58, 397–405. doi: 10.1001/archneur.58.3.397
- Moscoso, A., Silva-Rodríguez, J., Aldrey, J. M., Cortés, J., Fernández-Ferreiro, A., Gómez-Lado, N., et al. (2019). Prediction of Alzheimer's disease dementia with MRI beyond the short-term: implications for the design of predictive models. *Neuroimage Clin.* 23:101837. doi: 10.1016/j.nicl.2019.101837
- Petersen, R. C., Aisen, P. S., Beckett, L. A., Donohue, M. C., Gamst, A. C., Harvey, D. J., et al. (2010). Alzheimer's disease neuroimaging initiative (ADNI): clinical characterization. *Neurology* 74, 201–209. doi: 10.1212/WNL.0b013e3181cb3e25
- Royse, S. K., Minhas, D. S., Lopresti, B. J., Murphy, A., Ward, T., Koepp, R. A., et al. (2021). Validation of amyloid PET positivity thresholds in centiloids: a multisite PET study approach. *Alzheimers Res. Ther.* 13, 1–10. doi: 10.1186/s13195-021-00836-1
- Salvatore, C., Cerasa, A., Battista, P., Gilardi, M. C., Quattrone, A., Castiglioni, I., et al. (2015). Magnetic resonance imaging biomarkers for the early diagnosis of Alzheimer's disease: a machine learning approach. *Front. Neurosci.* 9:307. doi: 10.3389/fnins.2015.00307
- Scharre, D. W. (2019). Preclinical, prodromal, and dementia stages of Alzheimer's disease. *Pract. Neurol.* 15, 36–47.
- Schöll, M., Maass, A., Mattsson, N., Ashton, N. J., Blennow, K., Zetterberg, H., et al. (2019). Biomarkers for tau pathology. *Mol. Cell. Neurosci.* 97, 18–33. doi: 10.1016/j.mcn.2018.12.001
- Selkoe, D. J. (2001). Alzheimer's disease: genes, proteins, and therapy. *Physiol. Rev.* 81, 741–766. doi: 10.1152/physrev.2001.81.2.741
- Selnes, P., Aarsland, D., Bjørnerud, A., Gjerstad, L., Wallin, A., Hessen, E., et al. (2013). Diffusion tensor imaging surpasses cerebrospinal fluid as predictor of cognitive decline and medial temporal lobe atrophy in subjective cognitive impairment and mild cognitive impairment. *J. Alzheimers Dis.* 33, 723–736. doi: 10.3233/JAD-2012-121603
- Siafarikas, N., Kirsebom, B.-E., Srivastava, D. P., Eriksson, C. M., Auning, E., Hessen, E., et al. (2021). Cerebrospinal fluid markers for synaptic function and Alzheimer type changes in late life depression. *Sci. Rep.* 11:20375. doi: 10.1038/s41598-021-99794-9
- Smith, S. M., Jenkinson, M., Johansen-Berg, H., Rueckert, D., Nichols, T. E., Mackay, C. E., et al. (2006). Tract-based spatial statistics: voxelwise analysis of multi-subject diffusion data. *Neuroimage* 31, 1487–1505. doi: 10.1016/j.neuroimage.2006.02.024
- Smith, S. M., Jenkinson, M., Woolrich, M. W., Beckmann, C. F., Behrens, T. E., Johansen-Berg, H., et al. (2004). Advances in functional and structural MR image analysis and implementation as FSL. *Neuroimage* 23, S208–S219. doi: 10.1016/j.neuroimage.2004.07.051
- Ten Kate, M., Redolfi, A., Peira, E., Bos, I., Vos, S. J., Vandenberghe, R., et al. (2018). MRI predictors of amyloid pathology: results from the EMIF-AD multimodal biomarker discovery study. *Alzheimers Res. Ther.* 10, 1–12. doi: 10.1186/s13195-018-0428-1
- Tosun, D., Veitch, D., Aisen, P., Jack Jr, C. R., Jagust, W. J., Petersen, R. C., et al. (2021). Detection of β -amyloid positivity in Alzheimer's disease neuroimaging initiative participants with demographics, cognition, MRI and plasma biomarkers. *Brain Commun.* 3:fcab008. doi: 10.1093/braincomms/fcab008
- Zandifar, A., Fonov, V. S., Ducharme, S., Belleville, S., and Collins, D. L. (2020). MRI and cognitive scores complement each other to accurately predict Alzheimer's dementia 2 to 7 years before clinical onset. *Neuroimage Clin.* 25:102121. doi: 10.1016/j.nicl.2019.102121